

# Modulation of spatiotemporal dynamics of binocular rivalry by collinear facilitation and pattern-dependent adaptation

**Min-Suk Kang**

Department of Psychology and Vanderbilt Vision Research Center, Vanderbilt University, Nashville, TN, USA



**Sang-Hun Lee**

Department of Brain and Cognitive Sciences, Seoul National University, Seoul, South Korea



**June Kim**

Department of Brain and Cognitive Sciences, Seoul National University, Seoul, South Korea



**David Heeger**

Department of Psychology and Center for Neural Science, New York University, New York, NY, USA



**Randolph Blake**

Department of Psychology and Vanderbilt Vision Research Center, Vanderbilt University, Nashville, TN, USA, & Department of Brain and Cognitive Sciences, Seoul National University, Seoul, South Korea



The role of collinear facilitation was investigated to test predictions of a model for traveling waves of dominance during binocular rivalry (H. Wilson, R. Blake, & S. Lee, 2001). In [Experiment 1](#), we characterized traveling wave dynamics using a recently developed technique called periodic perturbation (M.-S. Kang, D. Heeger, & R. Blake, 2009). Results reveal that the propagation speed of waves for a collinear stimulus increased regardless of whether that stimulus was suppressed (replicating earlier work) or dominant; this latter finding is contrary to the model's prediction. In [Experiment 2](#), we measured perceptual dominance durations within a localized region in the center of two rival stimuli that varied in degree of collinearity. Results reveal that increased collinearity did not change average dominance durations regardless of the rivalry phase of the stimulus, again contrary to the model's prediction. Incorporating pattern-dependent modulation of adaptation rate into the model accounted for results from both experiments. Using model simulations, we show how interactions between collinear facilitation and pattern-dependent adaptation may influence the dynamics of binocular rivalry. We also discuss alternative interpretations of our findings, including the possible role of surround suppression.

Keywords: binocular rivalry, computational modeling, collinear facilitation, perceptual organization, perceptual dynamics

Citation: Kang, M.-S., Lee, S.-H., Kim, J., Heeger, D., & Blake, R. (2010). Modulation of spatiotemporal dynamics of binocular rivalry by collinear facilitation and pattern-dependent adaptation. *Journal of Vision*, 10(11):3, 1–15, <http://www.journalofvision.org/content/10/11/3>, doi:10.1167/10.11.3.

## Introduction

Neurons in primary visual cortex (V1) respond to contours of specific orientations falling within their receptive fields (De Valois, Albrecht, & Thorell, 1982; Hubel & Wiesel, 1962, 1968), but the strength of those responses can be substantially modulated by the concurrent presence of oriented contours falling outside the receptive fields of those neurons (Allman, Meizin, & McGuinness, 1985; Blakemore & Tobin, 1972; Maffei & Fiorentini, 1976). This contextual property of V1 physiology implies that neural signals depend on stimulus features beyond the boundaries of the conventionally

defined classical receptive field, and several mechanisms mediating these contextual influences have been described. One mechanism, termed surround suppression, entails a reduction in neural response strength once an optimum stimulus is enlarged beyond the boundaries of the classic receptive field (e.g., see synopsis by Smith, 2006). Putative perceptual consequences of surround suppression include reductions in apparent contrast (e.g., Xing & Heeger, 2001) and elevations in contrast detection and discrimination thresholds (e.g., Yu, Klein, & Levi, 2002). Another contextual mechanism, termed collinear facilitation, entails enhancement in neuronal responses to a target contour when that contour is accompanied by neighboring, collinear contours (Li, Piëch, & Gilbert, 2006), and here, too,

there are putative perceptual concomitants (e.g., Field, Hayes, & Hess, 1993; Kovács & Julesz, 1993). In this paper, we focus on contextual modulation within the context of binocular rivalry, i.e., the unpredictable alternations in perceptual dominance that occur when dissimilar images are presented separately to the two eyes (Levelt, 1965; Wheatstone, 1838).<sup>1</sup>

Numerous studies imply that rivalry dynamics are influenced by the spatial context in which rival stimuli appear. We know, for example, that multiple rival targets located in different parts of the visual field can engage in synchronized alternations when they share stimulus features such as color or contour orientation (Alais & Blake, 1999; Dörrenhaus, 1975; Kovács, Papathomas, Yang, & Fehér, 1996; Whittle, Bloor, & Pocock, 1968). Similarly, visual features located outside the boundaries of a rival target can influence the predominance of that rival target, as though the strength of the rival target were being modulated by its neighbors (Alais & Blake, 1998; Fukuda & Blake, 1992; Ichihara & Goryo, 1978; Mapperson & Lovegrove, 1991; Paffen, Tadin, te Pas, Blake, & Verstraten, 2006; Paffen et al., 2004). One particularly salient example of spatial interactions is revealed by the wave-like spread of dominance often seen during transition periods of binocular rivalry. To control where and when these traveling waves of dominance arise, Wilson, Blake, and Lee (2001) created spatially extended rival targets that confined the spatial path of these wave-like transitions and used brief contrast increments to control the location and time at which the transitions arose. With these stimuli and procedures, Wilson et al. were able to measure the speed with which waves of dominance emerged around a concentric rival target. They found that traveling waves propagated more rapidly when the contours forming the suppressed pattern were collinear with respect to the path of the wave.

To account for collinearity's effect on traveling waves, Wilson et al. proposed a simple model (see Figure 1) in which two layers of cortical units, each activated by one of the two rival stimuli, engage in reciprocal inhibition. This inhibition spreads through interneurons to adjacent units in the other layer, an arrangement that promotes recurrent disinhibition and, thereby, the spread of dominance over time. The units within a layer are interconnected with one another by reciprocal excitatory connections that mutually reinforce activity within neighboring units of a given layer. To account for the dependence of dominance wave speed on the spatial configuration of a rival target, these lateral, excitatory connections are more spatially extensive among units responsive to contours that are collinear, a property that promotes faster waves. To incorporate transitions from dominance to suppression states, the excitatory units in both layers (but not the inhibitory units) undergo neural adaptation in proportion to their activation levels. Simulations of that model were in good agreement with the speeds of traveling waves measured by Wilson et al. With the addition of an asymmetry in the interaction profiles

between the layers of neurons engaged in reciprocal inhibition, Knapen, van Ee, and Blake (2007) were able to generalize the Wilson et al. model to stimulus conditions where traveling waves of dominance were emerging during rivalry between stimuli rotating in opposite directions.

Although the model shown in Figure 1 was developed to account for the relatively fast spread of dominance of a collinear pattern as it emerged from suppression, this model also makes predictions pertaining to the spread of dominance within a suppressed pattern when the currently dominant pattern is collinear (i.e., when the collinear pattern is being engulfed by suppression over time). Based on intuition, one would expect a wave emerging from a suppressed stimulus to propagate more slowly when the currently dominant stimulus has strong collinearity, because neural responses within neurons representing that dominant stimulus are stronger as a consequence of the relatively strong excitatory connections among those neurons. Moreover, simulations of that stimulus condition using the Wilson et al. model produce results consistent with that intuition; those simulations are presented in the discussion of results from Experiment 1.

We tested this model prediction by measuring wave speed for different combinations of rival targets varying in

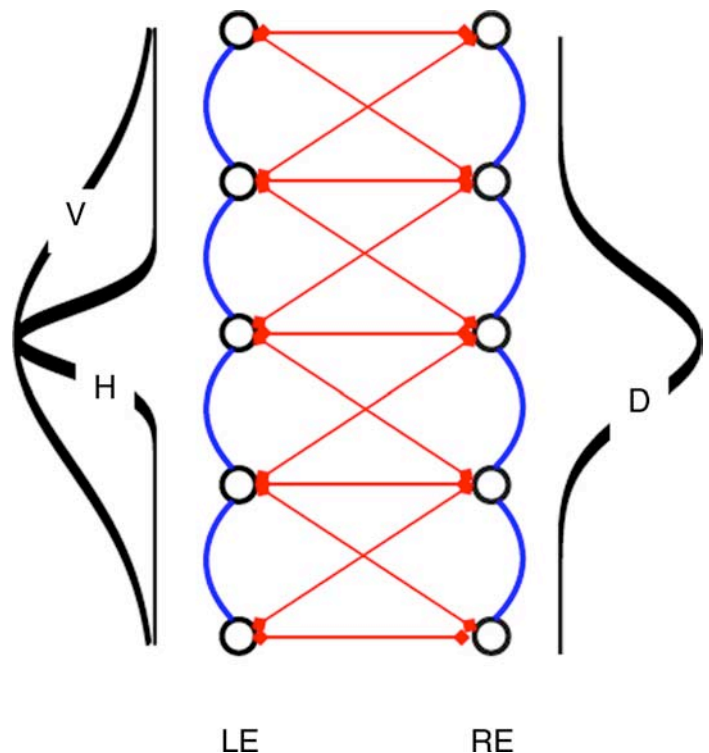


Figure 1. Schematic illustration of the model in which the two layers of neurons represent the two rival stimuli, respectively. The extent and the strength of recurrent excitation (shown in blue) associated with different contour orientations ( $V$  = vertical;  $D$  = diagonal;  $H$  = horizontal) are shown by the three Gaussian curves. Inhibitory connections are shown in red.

relative collinearity, and the results were surprising: a currently dominant rival pattern succumbs to suppression *more quickly* when its contours are collinear. This counterintuitive behavior can be accommodated within the collinear facilitation model proposed by Wilson et al. (2001) by the addition of a single parameter that governs the rate of buildup of pattern-dependent adaptation. In the [General discussion](#) section, we also explain why surround suppression, the other form of contextual modulation mentioned earlier, cannot explain the dependence of traveling waves on collinearity.

## Experiment 1

To measure pattern-dependent traveling wave dynamics during binocular rivalry, we used the periodic perturbation technique ([Figure 2a](#)) that was described and validated in a previous paper (Kang, Heeger, & Blake, 2009). The technique exploits the potency of a localized increment in contrast of the suppressed stimulus to promote local dominance and, moreover, for that local region of dominance to spread over neighboring areas of the visual field (Wilson et al., 2001). The traveling wave dynamics are inferred based on the observer's binary categorization of their perceptual experiences within a restricted region of the rival figure termed the monitoring region: perceptual switches at the monitoring region are delayed but time-

locked to the triggers, implying the existence of wave-like signals that propagate from the trigger site to the monitoring region. Using this technique, Kang et al. (2009) confirmed that the traveling waves of dominance of a stimulus emerging from suppression were faster when the contours comprising that stimulus were parallel to the path of the wave, not orthogonal.

The aim of [Experiment 1](#) was to examine the influence of the collinear facilitation within the currently dominant stimulus, and to achieve this aim, we prepared two stimulus conditions that yielded one of four possible traveling wave conditions ([Figure 2b](#)). A diagonal (D) grating was always presented to one eye and either a vertical (V) or a horizontal (H) grating was presented to the other eye. Within these vertically elongated stimuli, the V pattern comprised the high collinearity condition whereas the H pattern comprised the low collinearity condition. The lower region of [Figure 2b](#) illustrates two different traveling wave conditions associated with each pair of rival stimuli. Consider, for example, the situation where the rival stimuli were the D and V patterns (shown in the left column). In this situation, the emerging traveling waves appeared in the V pattern when the D pattern was perceptually dominant, and appeared in the D stimulus when the V pattern was perceptually dominant. Considering that the triggers were presented in anti-phase at the upper and lower regions of the two rival stimuli ([Figure 2a](#)), one of these waves propagated upward in response to the trigger given within the lower region of one eye and the other wave propagated downward in

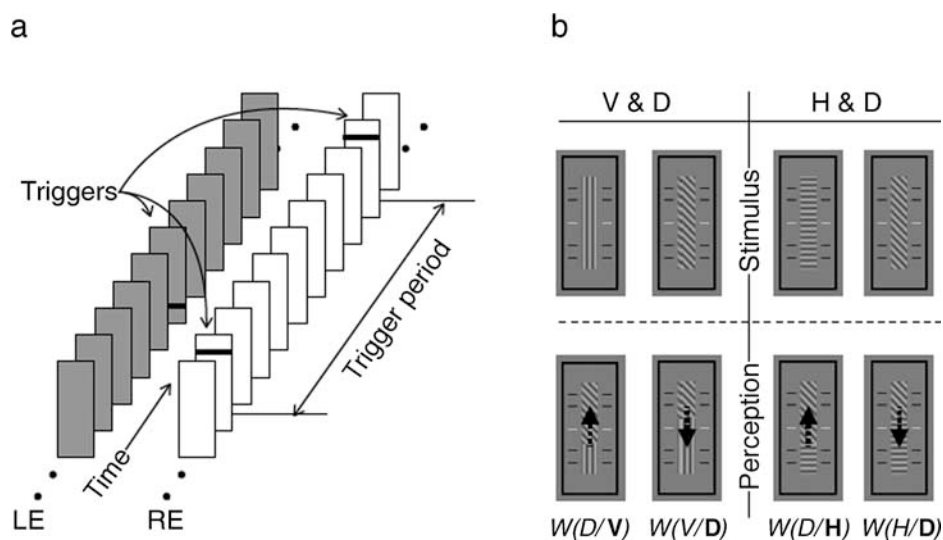


Figure 2. Stimulus conditions and procedure for [Experiment 1](#). (a) Stimulus sequence of periodic perturbation technique. Two vertically elongated rival stimuli are presented to the two eyes. One trigger is presented at the upper region of the left eye and another trigger is presented at the lower region of the right eye. These two triggers are presented in anti-phase and trigger period refers to the duration between the two trigger presentations within the same eye. (b) Stimulus conditions. The D pattern is always presented to one eye and either the H pattern or the V pattern is presented to the other eye (abbreviations designating these stimulus combinations are shown at the top). These two stimulus conditions, together with their associated triggers, produced four traveling wave conditions shown designated as follows:  $W(V/D)$ ,  $W(H/D)$ ,  $W(D/V)$ , and  $W(D/H)$ , where the bolded letter denotes the pattern receiving the trigger. Details are explained in the text.

response to the trigger given within the upper region of the other eye's stimulus. Similarly, dominance waves traveling in opposite directions could be triggered within the D and H rival stimuli.

In referring to these four types of traveling wave conditions, we will use the notation shown at the bottom of [Figure 2b](#), in which the first character indicates the dominant stimulus and the second character indicates the suppressed stimulus. To denote that the traveling waves emerge from the suppressed stimulus, the character denoting the suppressed stimulus is shown in bold, and we refer to this suppressed stimulus as the *carrier* of the wave. For example,  $W(D/V)$  refers to the condition where the initially dominant stimulus is the D pattern and it is the V pattern that emerges from suppression as a traveling wave of spreading dominance.

## Methods

All aspects of this study were approved by the Vanderbilt University Institutional Review Board. Six observers participated in this experiment (5 males, 1 female, average age 34 years old). Except for the first author and the last author of this paper, all other observers were naive to the purpose of the study. All had normal or corrected-to-normal vision, and all gave informed consent after thorough explanation of the procedures.

All stimuli and trial-related events were controlled by a Macintosh G4 computer (Apple, CA) running Matlab (Mathworks, MA) in conjunction with the Psychophysics Toolbox (Brainard, 1997; Pelli, 1997). Stimuli were presented on the screen of a Sony E540 21-inch monitor (1024 H  $\times$  768 V resolution; 120-Hz frame rate; 21.67 cd/m<sup>2</sup> mean luminance) in a dimly illuminated room. Stimuli were viewed against a gray background (21.67 cd/m<sup>2</sup>) through a mirror stereoscope placed 90 cm from the monitor.

Vertically elongated rival gratings ( $0.8^\circ \times 5^\circ$  visual angle, 4 c/deg) were presented to the left and right eyes ([Figure 2b](#)). To promote stable binocular alignment, each rival stimulus was bordered with a black rectangular frame ( $3.6^\circ \times 8^\circ$ ), the width of which was  $0.25^\circ$ . Five pairs of horizontal line segments ( $0.5^\circ$  in length) were presented at both sides of rival stimuli. Two pairs of them indicated the trigger locations (at  $\pm 1.5^\circ$  with respect to the center of the stimuli) and the central pair (colored white) designated the monitoring region (described below). Before the experiment, the contrast values of the rival stimuli were adjusted for each observer (15%–30%) to produce reasonably slow perceptual alterations (targeting a mean dominance duration of  $\sim 4$  s) and reliable traveling waves (Kang et al., 2009). As an aside, we also collected pilot data using horizontally elongated rival stimuli and obtained the same pattern of results as those produced by the vertically elongated stimuli; we chose to use vertical stimuli to minimize horizontal eye movements and to avoid hemifield differences.

Triggers were periodically presented at the upper and lower regions of each stimulus, respectively. Each trigger was presented for 200 ms with 100% contrast. Trigger period was individually adjusted from 3 s to 6 s. Observers were instructed to fixate the center of the stimuli (designated by the two white markers) and to monitor and track fluctuations in rivalry dominance within this region by pressing and holding either of two keys. Observers declared dominance only when one or the other of the rival gratings within the monitoring region was exclusively dominant, with neither key being pressed when mixtures were experienced. Each tracking session lasted 60 s and each test condition was repeated eight times. For each pair of rival stimuli (V and D; H and D), we randomly shuffled the order of the two trigger positions (upper left/lower right and lower left/upper right), the eye (left or right) receiving the D pattern, and the tilt (clockwise or counterclockwise from vertical) the D pattern.

## Results

Collinear contours promote faster traveling waves. [Figure 3a](#) shows the switch functions of the four traveling wave conditions, averaged across six observers. The switch function was obtained from the tracking record of the periodic perturbation technique, which represents the mean perceptual states as a function of trigger phase. The detailed procedure for obtaining this switch function is described elsewhere (Kang et al., 2009). In brief, the switch function is derived by averaging the time series of tracking records from the onset of one trigger to the onset of the other one. As shown in Kang et al. (2009), the switch function representing  $W(D/V)$  (blue solid line) is shifted leftward compared to the switch function representing  $W(D/H)$  (red solid line)<sup>2</sup>. This means that a pattern comprised of collinear contours exhibits faster traveling waves as it emerges from suppression, compared to a pattern composed of weakly collinear contours. This finding is entirely consistent with previous studies (Knapen et al., 2007; Wilson et al., 2001). However, the traveling waves emerging within the initially suppressed D pattern were also faster when that pattern was in rivalry with the collinear V pattern (condition  $W(V/D)$ , blue dotted line), compared to when the D pattern was in rivalry with the H pattern (condition  $W(H/D)$ , red dotted line). A collinear pattern, in other words, more quickly succumbs to suppression, contrary to expectation.

For purposes of statistical analysis, the latency of the waves was obtained from the switch function by estimating the threshold of a sigmoid fitted to the switch function (see details in [Appendix A](#)). In this measure, the latency reflects the time at which the perceptual states of both rival stimuli are balanced. [Figure 3b](#) shows latency associated with the four traveling wave conditions. Consistent with visual inspection of the switch functions ([Figure 3a](#)), the latencies obtained from those four traveling wave conditions show

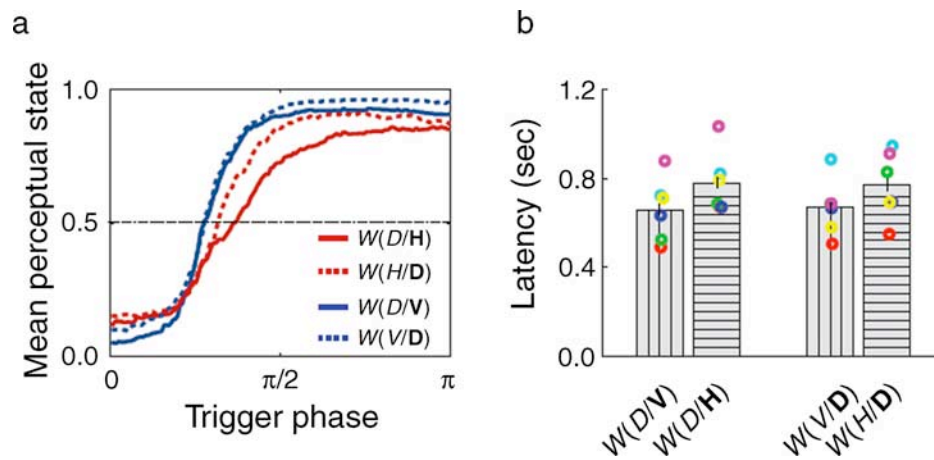


Figure 3. Results from Experiment 1. (a) Averaged switch functions from six observers. Four traveling wave conditions are indicated as follows. The blue lines represent the traveling waves arising from V and D rival patterns, and red lines represents the traveling waves arising from H and D patterns. Solid lines indicate the traveling waves emerging from V/H carrier whereas the dotted lines indicate the traveling waves emerging from D carriers (the term “carrier” refers to the pattern that is emerging from suppression into dominance consequent to presentation of a trigger at one end of that pattern). (b) Latencies for each of the four traveling wave conditions. The orientation of the fill pattern within each histogram signifies the stimulus pattern rivaling with D pattern. Colored circles indicate the individual data points, with a given color referring to a given observer. Error bars equal  $\pm 1$  SE.

that traveling waves propagated faster when rivalry was between the D and V patterns relative to rivalry between the D and H patterns, irrespective of which stimulus was the carrier of the traveling waves. A repeated measure of two-way ANOVA with the factors of carrier pattern (V/H and D) and collinearity (V and H) revealed that the effect of collinearity was statistically significant [ $F(1, 5) = 23.90, p < 0.01$ ], but the effect of the carrier pattern was not significant [ $F(1, 5) \sim 0, p \sim 1$ ]. This result was evident for all observers (Figure 3b, each color represents a different observer). Latencies obtained by estimating the time point at which the switch function passes the mean perceptual state (0.5) produced similar results, again contrary to expectation.

Experiment 1 confirms that the speed of the emerging traveling waves depends on the degree of collinearity of the rival targets, but this is true regardless of the perceptual state of the collinear pattern. We find, in other words, that a stimulus dominant in rivalry is more susceptible to spreading suppression when that stimulus consists of contours that are collinear. In the following paragraphs, we will show that this outcome is inconsistent with predictions from the collinear facilitation model proposed by Wilson et al. (2001). Moreover, we will show how a simple modification to that model brings its predictions in line with these seemingly counterintuitive results. That modification involves the addition of a parameter that governs the rate of pattern-dependent adaptation. To start, we need to explain the rationale for pattern-dependent adaptation in the original model.

First, it is well-known that exposure, or adaptation, to a pattern temporarily reduces the effective contrast of that pattern, with the magnitude of this reduction in effective contrast proportional to the contrast experienced during

adaptation (Blakemore, Muncey, & Ridley, 1973; Greenlee, Georgeson, Magnussen, & Harris, 1991). Stronger contrast, in other words, produces more robust adaptation, presumably attributable to the stronger neural responses associated with higher contrast stimulation. In contemporary parlance, contrast adaptation is a by-product of contrast gain control (e.g., Heeger, 1992), a component of which seems to operate prior to the level of binocular rivalry (Watanabe, Paik, & Blake, 2004). It is reasonable to expect, therefore, that collinear facilitation could boost the stimulus strength of a pattern and, thereby, increase the magnitude of self-adaptation associated with viewing that pattern. Second, it is commonly believed that contrast adaptation plays an important role in triggering switches in dominance during binocular rivalry (Shapiro, Moreno-Bote, Rubin, & Rinzel, 2009; Wilson, 2007), and we know that adaptation to a pattern prior to the onset of rivalry (Blake & Overton, 1979; Wade & de Weert, 1986) or intermittently during ongoing rivalry (Kang & Blake, 2010) reduces the dominance of that pattern during rivalry.

Combining these ideas about adaptation and applying them to the conditions of rivalry used in the present paper, we see that collinearity can produce two opposing influences on the strength of a rival target. On the one hand, neural activity associated with a collinear pattern (i.e., the V stimulus) should be stronger owing to the recurrent excitatory connections among neurons registering the presence of that pattern. On the other hand, those stronger neural responses should produce greater self-adaptation of that collinear stimulus. To confirm how these two factors might operate for perception of traveling waves during binocular rivalry, we implemented the model proposed by Wilson et al. (2001) to account for traveling waves. In the following section, we

present results from simulations of that model showing that it fails to account for the results of [Experiment 1](#). We then show that those results can be accommodated by adding a single parameter to the model, one that controls the time course of adaptation in a pattern-dependent manner.

## Simulation of traveling waves

We adapted the network model shown schematically in [Figure 1](#) to the conditions of rival stimulation used in our studies. In our instantiation of the model, the dynamics of traveling waves are governed by the following equations:

$$\tau_E \partial_t E_{Aj} = -E_{Aj} + \frac{[P_{Aj}]^2}{(10 + H_{Aj})^2 + [P_{Aj}]^2}, \quad (1)$$

$$P_{Aj} = S_{Aj} - \eta_I \sum_{k=1}^N \varphi_{Bjk} I_{Bk} + \eta_E \sum_{k=1}^N \varepsilon_{Ajk} E_{Ak}, \quad (2)$$

$$\varphi_{Ajk} = \exp\left(\frac{-(k-j)^2}{4\sigma_\varphi^2}\right), \quad (3)$$

$$\varepsilon_{Ajk}(X) = \exp\left(\frac{-(k-j)^2}{4\sigma_\varepsilon(X)}\right) (k \neq j) \quad (4)$$

in which  $X$  is the stimulus pattern,

$$\tau_I \partial_t I_{Aj} = -I_{Aj} + E_{Aj}, \quad (5)$$

$$\tau_H \partial_t H_{Aj} = -H_{Aj} + \eta_H \gamma_{AH} E_{Aj}, \quad (6)$$

$$\gamma_{AH} = 1 + g(X) \text{ in which } X \text{ is the stimulus pattern.} \quad (7)$$

Subscripts  $A$  and  $B$  represent the two eyes, respectively,  $X$  is the stimulus pattern, and  $j$  indicates the  $j$ th neuron among those  $N$  units (40 in our implementation of this

model) representing vertically elongated stimuli presented to the left and right eyes.  $E$  represents the rate of neural activity governed by [Equation 1](#), in which the time constant  $\tau_E$  equals 20 tu (tu refers to time unit, which is arbitrary);  $H$  is the term embodying spiking adaptation. Each unit in the network receives an input  $P$  whose value is determined by stimulus strength  $S$  ( $=30$ ), by subtractive inhibition from neighboring cells representing the stimulus presented to the contralateral eye and by additive recurrent excitation from neighboring cells representing the stimulus presented to the same eye. The notation  $[P]$  is the maximum operator applied to the external input that compares  $P$  and 0 and returns the larger value. In this simulation, the extent of reciprocal inhibition is governed by [Equation 3](#), in which the constant  $\eta_I$  is equal to 0.1 and  $\sigma_\varphi$  is equal to 1.5 irrespective of rival stimuli. In contrast, the extent of recurrent excitation governed by [Equation 4](#) changes depending on the pattern of the rival stimulus, with  $\sigma_\varepsilon$  equaling 2 for H stimulus, 2.5 for D stimulus, and 3 for V stimulus. The constant  $\eta_E$  was set to 0.04 for this simulation. [Equation 5](#) determines the inhibition for which  $\tau_I$  is set to 11 tu. Slow adaptation is governed by [Equation 6](#) in which  $\tau_H$  was set to 900 tu and adaptation rate  $\eta_H$  equaled 0.3 (see other details in [Appendix A](#)).

In this model, as in the original version, the magnitude of recurrent excitation decreases differentially depending on the collinearity of rival stimulus, such that the magnitude of collinear facilitation falls off more slowly with increasing distance for the V pattern (collinear in our stimulus configuration) compared to the H pattern (weaker collinearity). The extent of inhibition is symmetrical regardless of the rival pattern. In the original Wilson et al. model, adaptation magnitude, as embodied in the parameter  $H$ , is dependent on activity level  $E$  ([Equation 6](#)), and  $E$  is dependent on collinearity. Thus, increased activity level accompanied by collinear facilitation increases the magnitude of adaptation. There was no variable, however, governing rate of adaptation, meaning that rate was independent of pattern collinearity. We have added a rate parameter  $\gamma$  ([Equation 6](#)) whose value can vary with collinearity according to the variable  $g(X)$ . Note that when the parameter value for  $\gamma$  is set to 1.0 (i.e.,  $g(X) = 0$ ), the modified model is identical to the original Wilson et al. model (i.e., rate is invariant with pattern). The time course of adaptation is slower relative to the original Wilson model when  $\gamma$  is less than 1.0 (i.e.,  $g(X) < 0$ ) and is faster when  $\gamma$  is greater than 1.0 (i.e.,  $g(X) > 0$ ).

We first verified that the model (when modified for our stimulus conditions) produced traveling waves under conditions embodied in the periodic perturbation technique. [Figure 4a](#) shows how simulated neuronal activity fluctuates over time in response to repeated triggers presented alternately to a pair of rival targets composed of diagonally oriented contours oriented leftward for one eye and rightward for the other eye. In this simulation, the extent and magnitude of collinear facilitation for the two rival stimuli are the same to simulate the traveling waves

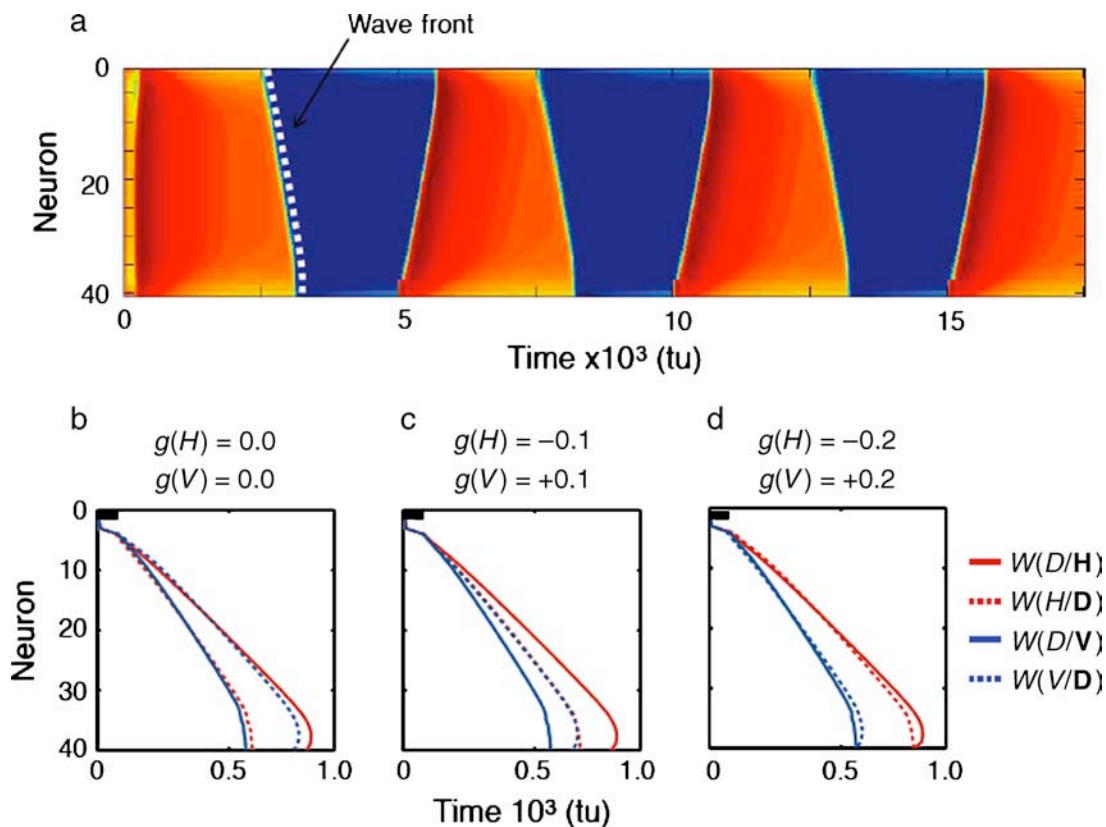


Figure 4. Model simulations for Experiment 1. (a) Simulation result of periodic perturbation between two, orthogonally oriented D rival patterns, with color representing the activity levels of the 40 neurons forming the rivalry network (recall Figure 1). Triggers are presented every 2500 tu (tu means time unit, which is arbitrary) in anti-phase between the two eyes, resulting a 5000-tu trigger period. The white dotted line illustrates the *wave front* that is obtained by connecting the same activity level of all neurons over time. This wave front indicates that perceptual switching occurs sequentially across this array of 40 neurons, producing a traveling wave of changing dominance state. (b–d) The wave fronts associated with four traveling wave conditions with varying degrees of adaptation rate. The legend designating these four conditions is shown at the right side of (d).

arising from these two orthogonally oriented, diagonal patterns. Triggers were given every 2500 tu, meaning that the trigger period was set to be 5000 tu in this simulation. As mentioned above, the network comprised 40 neurons, and for this simulation the triggers were introduced among the first 3 and last 3 neurons by briefly (125 tu) increasing the stimulus strength twofold within those units. In response to each trigger given during the suppression phase of a rival stimulus, a traveling wave was indeed induced as evidenced by the successive, abrupt changes in activity over serially connected neurons (note that the first trigger was given at 2500 tu). We characterize the spatiotemporal modulation in network activity as the *wave front* of the traveling wave, and one example of such a wave front is indicated by the white dotted line in Figure 4a. This wave front was defined by the series of time points among the array of neurons when their activity levels reach an arbitrary, fixed value ( $E = 30$ ). The regularity of this wave front behavior seen in Figure 4a arises, of course, because the perturbations producing the spreading state transitions

defining the wave fronts are themselves periodic. The time elapsing between the presentation of a trigger within one extreme of the network and the arrival of the resulting wave front at the other extreme of the network defines the speed of the traveling wave. The simulation shown in Figure 4a confirms that this instantiation of the reciprocal inhibition model proposed by Wilson et al. produces reliable traveling waves under conditions of periodic perturbation. We next will use this wave front concept to test the effect of different stimulus configurations on the speed of waves.

We start with simulations where the adaptation rate is assumed to be constant regardless of pattern collinearity (i.e., where  $\gamma = 1.0$  because  $g = 0$ )—this assumption represents the way adaptation is implemented in the original version of the Wilson et al. model. The resulting wave fronts are shown in Figure 4b. As produced by the original version of that model (Wilson et al., 2001), traveling waves emerging from the V carrier (solid blue line) are faster than those emerging from the H carrier (solid red line); this outcome is

consistent with results from earlier traveling wave studies (Kang et al., 2009; Wilson et al., 2001). Next, consider how the model with invariant adaptation rate behaves when the simulated traveling waves emerge from the D pattern (dotted lines in Figure 4b). Here the model simulation produces waves that emerge faster when the D pattern rivals with the H pattern than when it rivals with the V pattern. This outcome corresponds to the intuitive prediction described in the Introduction section, but it does not correspond to the actual results: in fact, the D pattern emerges more quickly when overcoming suppression exerted by the V pattern (recall Figure 3b, right-hand pair of histograms).

The model's behavior can be brought into compliance with the empirical results simply by varying adaptation rate dependent on collinearity. To reiterate, adaptation rate is defined as adaptation constant ( $\eta_H$ ) multiplied by  $\gamma$ :  $\gamma = 1 + g(X)$ , in which the term  $g(X)$  represents the modulation factor dependent on the degree of collinearity of the pattern  $X$ . The modulation factor reflects pattern-dependent adaptation such that  $g(V)$  always equals or is greater than 0, and  $g(H)$  always equals or is less than 0, whereas  $g(D)$  equals 0 for all conditions. Implemented in this way, adaptation rate is highest for V and lowest for H, with D being intermediate. The consequence of this modification to the model can be seen in Figures 4c and 4d, which correspond to two different sets of values for the parameter  $g$  that modulates the adaptation rate  $\gamma$ . Notice that the model continues to produce the well-established speed difference between collinear and orthogonal contours (vertical and horizontal in this case) emerging from suppression: the wave front defined by the solid blue line always intersects the  $x$ -axis (time) at a point well to the left of the intersection time for the wave front defined by the solid red line. Now, however, the traveling waves, represented as the wave fronts, associated with emergence of the D pattern into dominance changes when values of  $g(V)$  or  $g(H)$  change across Figures 4b–4d: the D pattern waves are faster (as indicated by the leftward shift in the blue dotted line) when that D pattern is in rivalry with the V pattern but slower (as indicated by the rightward shift in the red dotted line) when the D pattern is in rivalry with the H pattern.

These simulation results thus show that incorporation of pattern-dependent adaptation rate into the model shown schematically in Figure 1 enables that model to produce the seemingly counterintuitive influence of collinearity on emerging waves of dominance. Now, from our earlier work (Kang et al., 2009) we know that the spatiotemporal dynamics of traveling waves are closely related to the spontaneous perceptual alternations during binocular rivalry. This led us to hypothesize that the interaction between collinear facilitation and pattern-dependent adaptation should also be reflected in the durations of dominance measured under conditions where perceptual alternations occur spontaneously, with no external influences caused by perturbation triggers. Experiment 2 tests this prediction.

## Experiment 2

In binocular rivalry, a stronger (e.g., higher contrast) stimulus typically enjoys enhanced perceptual dominance (e.g., Levelt, 1965). Combining this property of binocular rivalry with the putative strengthening influence of collinear facilitation, one might expect that the V pattern competing with the D pattern would show stronger perceptual dominance than the H pattern competing with the D pattern. Yet there are published results contrary to this expectation. Specifically, Alais, Lorenceau, Arrighi, and Cass (2006) measured concurrent perceptual dominance of two pairs of rival stimuli, i.e., a pair of spatially separated 1D Gabor patches presented to one eye in competition with a pair of noise patterns presented to the other eye. The concurrent perceptual dominance (i.e., synchronization of dominance states) of the two Gabors increased with their degree of collinearity. However, Alais et al. found that the perceptual dominance (indexed by mean dominance duration) of the individual rival gratings did not vary with collinearity, contrary to what would be expected based on the putative enhanced strength of collinear contours. Based on this odd result, Alais et al. concluded that “the rivalry processes do not impinge upon the contour association strengths” (p. 1485). In view of the results and implications from Experiment 1, however, we realized that this odd failure for collinear stimuli to predominate in rivalry might have something to do with interactions between collinear facilitation and stimulus pattern-dependent adaptation, leading us to perform this next experiment.

## Methods

Elongated stimuli like those used in Experiment 1 were used for these measurements. Five of six observers who participated in Experiment 1 (including the first author and the last author) also participated in Experiment 2. As before, observers tracked periods of exclusive rivalry dominance of a given rival target (H, D, or V) within the monitoring region of the stimuli during 60-s tracking periods. (These measurements were actually performed in the context of a larger set of conditions in which small gaps were placed in one of the two rival stimuli, but those gap conditions are not relevant for the predictions we are examining here.) Now, however, there were no external perturbations to trigger traveling waves; we measured successive durations of dominance produced by spontaneous transitions in rivalry state. Because the monitoring region was quite small, mixture periods were brief and infrequent, and consequently, we considered only the periods of exclusive dominance of the gratings within the monitoring region for analysis. As in Experiment 1, a D (diagonal) pattern was presented to one eye and either a V pattern (vertical: high collinearity)



or an H pattern (horizontal: low collinearity) was presented to the other eye. A given rival condition was repeated four times, and the eye receiving the diagonal stimulus was counterbalanced.

## Result

Figure 5 shows the mean dominance durations from four stimulus patterns associated with two pairs of rival stimuli (V and D; H and D). Pairwise comparisons reveal no statistically significant differences in the dominance durations associated with rivalry between the V and D patterns [ $F(1, 4) = 0.05, p > 0.5$ ] nor for the H vs. D patterns [ $F(1, 4) = 2.24, p \sim 0.2$ ]. Of particular relevance for our purposes, the average dominance durations of the V pattern and of the H pattern are not significantly different [ $F(1, 4) = 4.78, p \sim 0.09$ ], even though both V and H patterns were in rivalry with the same D pattern. This pattern of results is reminiscent of the puzzling finding reported by Alais et al. (2006).

It is important to note that our results do not necessarily indicate that vertical, diagonal, and horizontal contours are equally strong rival targets; indeed, there is mixed evidence in the rivalry literature concerning the effect of contour orientation on binocular rivalry. Wade (1974, 1975) found no significant differences between predominance of vertical over horizontal contours, while Fahle (1982) found that horizontal rival gratings were signifi-

cantly weaker compared to vertical or, for that matter, compared to diagonally oriented rival gratings. In those earlier studies, however, vertical and horizontal rival targets were *equally* collinear because the rival targets were either single lines (Fahle, 1982; Wade, 1974) or were circular gratings. Recall, too, that results from our pilot experiment replicated the results shown in Figure 3 using horizontally elongated rival target configurations in which horizontally oriented contours are the most highly collinear. The effects described in this paper, in other words, pertain to collinearity, not orientation.

Finally, our results do not mean that the predominance of stronger rival target is no greater than the predominance of weaker rival target. It is a common assumption in rivalry models, including variants of the one being tested in our paper, that reciprocal inhibition between neural representations of rival stimuli, in addition to adaptation, play a role in governing predominance; the strengths of those inhibitory interactions are modulated by the adaptation states of neurons activated by the dominant stimulus and by neurons activated by the suppressed stimulus. Moreover, it is now generally thought that “noise” also represents an important ingredient governing rivalry alternations, a point we return to in the next section of the paper. So it would be the interaction of collinearity with those other factors that would govern dominance durations of spatially extended rival patterns (like ours) or spatially neighboring rival patterns (like those used by Alais et al.). Are the interactions embodied in the modified version of the Wilson et al. model able to predict the dominance durations measured in our Experiment 2? The simulations described in the next section provide an affirmative answer to that question.

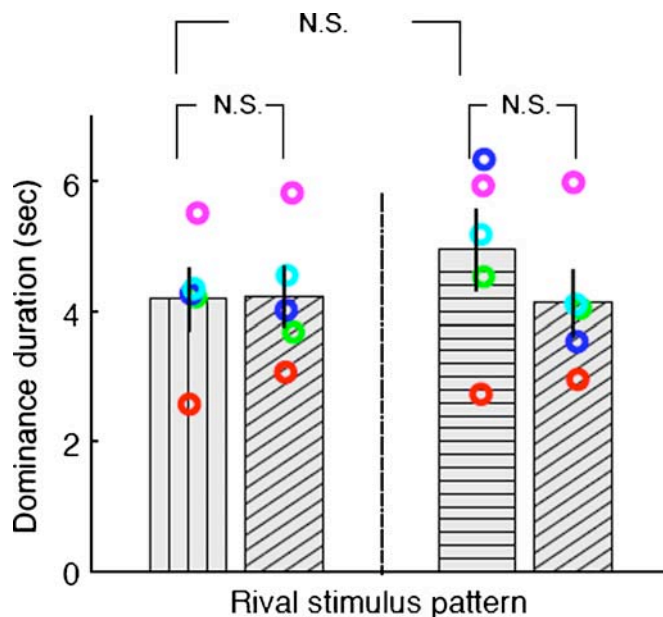


Figure 5. Results from Experiment 2. Average dominance durations for four stimulus conditions, corresponding to two pairs of rival patterns (V and D; H and D). The orientation of the fill pattern within each bar signifies the stimulus pattern. Error bars indicate  $\pm 1$  SE and colored circles indicate data for a given observer.

## Simulation of rivalry dynamics

Simulations were performed in which we varied the extent of recurrent excitation and pattern-dependent adaptation gain to learn how these two mechanisms interact to influence predicted rivalry dominance values. We used the same set of equations that embody interactions among an array of 20 units representing the vertically elongated region of the visual field within which the two rival patterns were imaged. In this simulation, unlike the previous one for Experiment 1, we did not provide external triggers to promote periodic switches in rivalry state because in Experiment 2 switching occurred spontaneously, not because of periodic perturbation. To produce realistic alternations in rivalry state in the absence of externally triggered switches, we added a Gaussian noise term in Equation 2 (see details in Appendix A). The inclusion of noise to promote spontaneous alternations comports with the widely accepted assumption that spontaneous alternations in dominance involve both neural adaptation and noise (Kang & Blake, 2010; Lankheet, 2006; Lehky, 1988; Moreno-Bote, Rinzel,

& Rubin, 2007; Shpiro et al., 2009; but see Wilson, 2005, for a discussion of models that, in principle, can produce alternations without noise). Van Ee (2009) provides an excellent description of the ways that noise might influence rivalry alternations, including ideas about exactly where in the process noise exerts its influence.

Figure 6 shows the results from our simulations. Figure 6a shows how simulated average dominance

durations for the V rival pattern (solid lines) and the D rival pattern (dotted lines) vary as a function of adaptation rate of the V pattern, i.e.,  $g(V)$ ; the adaptation rate for the D pattern remains constant. The different colored lines denote stimulus conditions in which the V pattern is assigned different values of  $\sigma_\epsilon$ , i.e., different degrees of recurrent excitatory spread of the V pattern (shown by the colored gradients within the figures). When  $g(V)$  is 0,

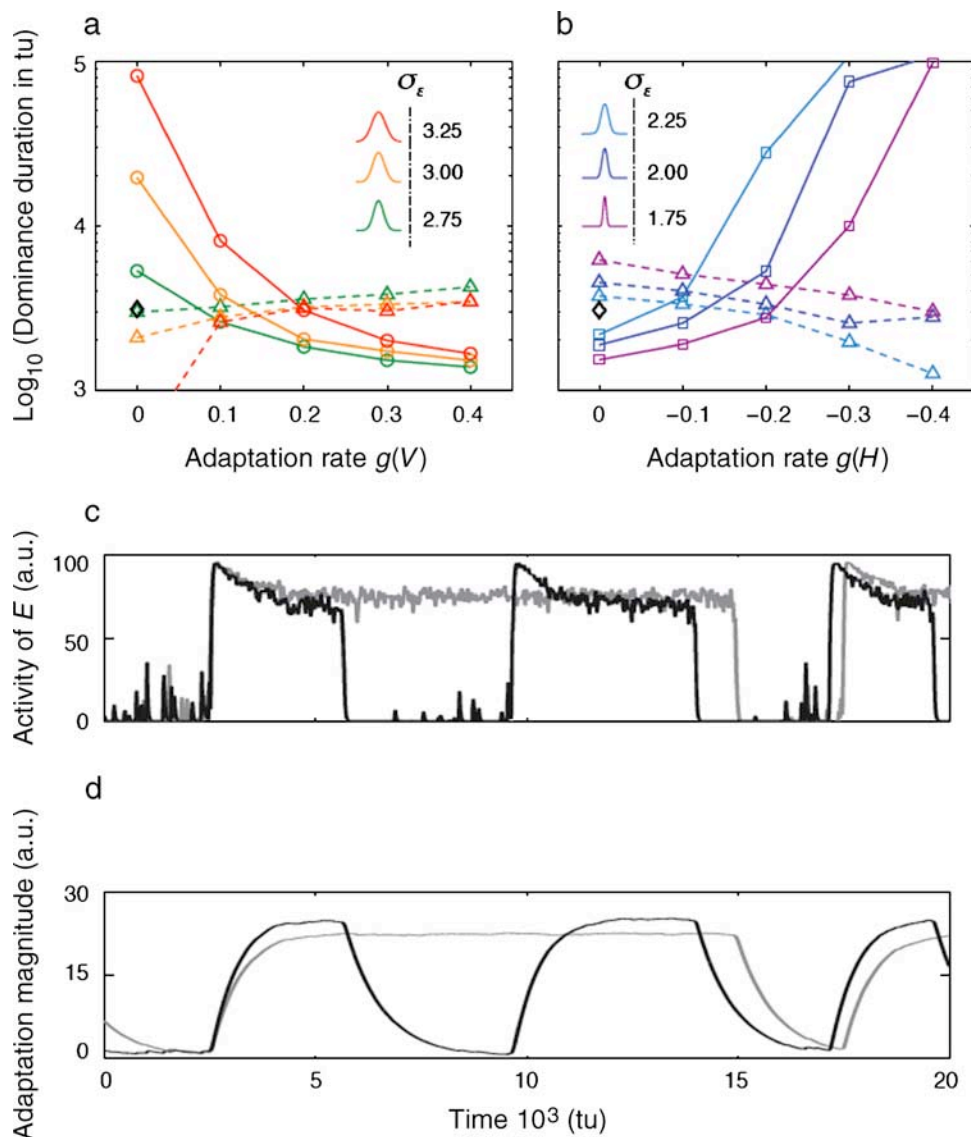


Figure 6. Model simulations for Experiment 2. Simulated dominance durations for (a) a V pattern (circles connected by solid lines) and (b) an H pattern (squares connected by solid lines) in rivalry with a D pattern, as a function of adaptation rate (expressed in terms of the value of  $g$  plotted along the x-axis). Also plotted are simulated dominance durations for the D pattern (triangles connected by dotted lines) when it is in rivalry (a) with the V pattern and (b) with the H pattern. The parameter is an extent of excitatory spread ( $\sigma_\epsilon$ ), and the different simulated values are plotted in different colors as signified by the figure inserts. Excitatory spread for the D pattern is invariant ( $\sigma_\epsilon = 2.5$ ); the different colored dotted lines denote simulated dominance values for the D pattern dependent on the spread parameter for the V and for the H patterns in rivalry with the D pattern. The single, black diamond symbol in each panel shows the simulated dominance durations when two orthogonally oriented D patterns are engaged in rivalry. (c, d). Simulated activity level and adaptation level for a model unit located within the middle of the array representing a vertically elongated V rival pattern. (c) Activity of the model unit with a fixed collinear facilitation parameter ( $\sigma_\epsilon = 3.0$ ), simulated using two different values for pattern-dependent adaptation rate (gray for  $g = 0.0$  and black for  $g = 0.2$ ). (d) Adaptation level within this model neuron. The color (adaptation rate) and the time course are matched with (c).

adaptation rate is 1 (i.e., the original version of the Wilson et al. model); for these parameter values, the simulated dominance durations associated with the V pattern increase and dominance durations of the D pattern decrease as the spatial extent of recurrent excitation broadens. Of particular relevance, note that predicted dominance durations for V are always longer than predicted durations for D, an outcome that, in fact, is not observed empirically (recall Figure 5 and the results from Alais et al., 2006). For non-zero values of  $g(V)$ , however, simulated dominance durations of the V pattern systematically decrease whereas simulated dominance durations of the D pattern increase. Note that there is a value of  $g(V)$  where the dominance durations for the D and V patterns are comparable, i.e., the pattern of results found by us and by Alais et al. (2006). Figure 6b shows the same pattern of results for simulations of dominance durations for rivalry between the H pattern (solid lines) and the D pattern (dotted lines). Now when  $g(H)$  is 0 (i.e.,  $\gamma = 1.0$ ), dominance durations for the H pattern are consistently less than dominance durations for the D pattern, contrary to our findings. For non-zero values of  $g(H)$ , dominance durations for D and for H patterns are inversely affected, and once again there is an adaptation rate value at which those two patterns produce comparable simulated dominance durations. The patterns of simulated results in Figures 6a and 6b thus confirm that pattern-dependent adaptation rate brings the behavior of this model in line with empirical results. Moreover, it is worth noting that the values of  $g(V)$  and  $g(H)$  that yield comparable dominance durations for V and D patterns and for D and H patterns, respectively, approximate the values of  $g(V)$  and  $g(H)$  that reproduce the traveling wave speed results from Experiment 1 (see Figure 4d).

To envision how collinear facilitation and pattern-dependent adaptation jointly influence the behavior of a model neuron within the array representing a rival target, we extracted the simulated activity of the 10th model neuron ( $E_{10}$ ), representing the V pattern when paired against the D pattern in rivalry. Figure 6c shows that unit's activity over time for two different values of  $g(V)$ ; the value of the collinear facilitation parameter was held constant at  $\sigma_\varepsilon = 3.0$ . The activity of this model neuron with fast adaptation rate (black trace, for the condition  $g = 0.2$ ) rises quickly upon a transition and then quickly begins to descend to a level lower relative to the activity of a model neuron with  $g = 0$  (gray trace). This quick drop in activity level in the model unit results from the time course of adaptation within that unit, which is shown in Figure 6d. Here it can be seen that the value of  $H$  (level of spiking adaptation; see Equation 6) rises more quickly and to a higher level for the non-zero value of  $g$  (black trace) compared to adaptation when  $g$  is zero (gray trace). As a consequence, the stronger adaptation and, hence, weaker activity level of this unit renders it more susceptible to abrupt state changes in the model because of its increased vulnerability to intrinsic noise. This behavior is consistent

with the putative role of noise in the production of dominance state changes during binocular rivalry (Kang & Blake, 2010; Lankheet, 2006; Moreno-Bote et al., 2007; Shpiro et al., 2009).

## General discussion

To explain the counterintuitive results of Experiments 1 and 2, we have posited that pattern-dependent adaptation operates together with collinear facilitation, and we provided computational evidence showing that a model incorporating those elements could produce rivalry dynamics mirroring our counterintuitive results. The incorporation of an additional model parameter governing adaptation rate is an unusual proposal and, while not without precedent (Rezec, Krekelberg, & Dobkins, 2004), does place the onus on us to demonstrate that other, potentially more parsimonious explanations can be ruled out.

One referee of an earlier version of this paper pointed out that the speed of apparent motion (AM) produced by briefly presented, spatially separated visual elements appears faster when those elements comprise collinear stimuli compared to orthogonal ones and when those implied speeds are very high (Georges, Seriès, Frégnac, & Lorenceau, 2002). Our stimuli, of course, do not involve AM, but we and others (Wilson et al., 2001) certainly do find that traveling waves emerge faster from a suppressed stimulus that comprises collinear contours. The speed of those traveling waves, however, is almost an order of magnitude slower than the optimal speed evoking the illusory increase in speed of briefly flashed AM sequences (Georges et al., 2002). Moreover, the present experiments reveal that waves of dominance also emerge more rapidly when the highly collinear rival target is the currently *dominant* one that is succumbing to suppression. The emerging wave, in other words, is being carried on a more weakly collinear pattern, meaning that AM cannot explain the faster traveling waves from V and D rival stimuli regardless of carrier. In addition, to explain our result requires assuming that the substrate determining wave perception is independent of the eye receiving the pattern in which the wave emerges. That seems highly unlikely since the waves are being repetitively triggered in left- and right-eye stimuli by monocularly presented trigger stimuli; if eye of origin did not matter, then the periodic perturbation technique would not work in the first place.

Next we need to reconsider the other form of contextual modulation mentioned in the Introduction section, surround suppression, which has been invoked in other studies involving short duration binocular rivalry (Bonneh & Sagi, 1999) and, possibly, implicated in studies of extended duration binocular rivalry (e.g., Paffen et al., 2006, 2004). The stimulus configuration and procedure

used in our experiments (Figure 2a) differ in important ways from those previous studies. For one thing, our rival stimuli were presented for many seconds, not a fraction of a second as done by Bonneh and Sagi (1999). Moreover, our stimuli allowed us explicitly to separate effects of surround and collinearity; surround conditions in Paffen et al.'s (2004) study always involved collinear contours. Likewise, in condition b in Paffen et al. (2006) the surround stimuli were identical in both eyes (only rival targets differed in orientation), unlike in our present study. Specifically, we required observers to monitor the rivalry state of a central region flanked above and below by additional rival stimulation identical to that within the monitoring region. It is reasonable, therefore, to assume that the effective contrast of the contours within this central region could be affected by the surrounding contours. However, as pointed out earlier, for all of these rival configurations—V, H, and D—the contour orientation within the central region is identical to the contour orientations within the flanking regions. So to the extent that surround suppression is dependent on relative orientations between center and surround, there should be no differential influence on the effective contrast of the central, monitoring region. In addition, to the extent that surround suppression also includes a non-oriented component (e.g., Meese, Georgeson, & Baker, 2006), we would expect the relative orientations of central and flanking regions not to matter for the degree of suppression arising from that component. In short, we see no way to predict the pattern of results obtained in our two experiments based on known properties of surround suppression. One would have to posit the existence of orientation-selective suppression that operates such that the surround portion of one eye's stimulus exerts its strongest effect on the central region of the other eye's stimulus. Single-unit recordings from macaque V1 clearly contradict such a suppression scheme (Webb, Dhruv, Solomon, Tailby, & Lennie, 2005).

Moreover, it is striking to compare the results from contrast matching experiments using stimulus configurations similar to those used in the present study, for those studies indicate that surround suppression should be the same for what we are calling “high collinearity” and “low collinearity”. Specifically, Xing and Heeger (2001) show evidence for surround suppression when test and surround are equal in contrast (as they are in our study), and furthermore, the magnitude of that suppression was the same for a “high collinearity” configuration and a “low collinearity” configuration. Similarly, Ejima and Takahashi (1985) found no difference in suppression strength between high and low collinearity conditions when the contrast of the central portion of their test grating was equal to the contrast within the flanking grating regions. Now it is true that these suppressive effects can be replaced by facilitation effects, but this typically occurs only at very low flanker contrast levels, whereas our rival stimuli

always had the same contrasts throughout their entire extent.

That said, we realize that surround suppression can play a role in modulating the effective contrast in regions within spatially extensive rival configurations, and we acknowledge that future modeling work should take into account the effects that those modulations may have in governing contrast gain control during binocular rivalry.

To end on a speculative note, it is natural to wonder about the possible functional significance of pattern-dependent adaptation, i.e., the mechanism necessary to bring the Wilson et al. model in line with our results. Barlow and Földiák (1989) have proposed that adaptation serves to decorrelate neural responses, thereby promoting more efficient neural coding. We typically think of adaptation in terms of statistical dependency over time (e.g., the continued presence of a given pattern), but collinearity also represents an example of statistical dependence, in this case over space. Indeed, statistical analyses of the co-occurrence of edge elements within natural visual scenes reveal that neighboring collinear contours abound (Geisler, Perry, Super, & Gallogly, 2001). To the extent that adaptation operates to promote greater statistical independence within neural elements responsive to collinear contours, it stands to reason that strong spatial dependency among image contours would affect adaptation. In addition, a rate-dependent parameter on that adaptation process would insure that optimization happens fastest for those highly likely configurations.

## Conclusion

A number of stimulus factors influence perceptual alternations during binocular rivalry, including contrast, spatial frequency, orientation, motion, stimulus complexity, and top-down influences including attention (see Blake & O'Shea, 2009, for an overview of those factors, and Kang, 2009, for a detailed explication of the spatiotemporal properties of rival stimulation). The present results, including model simulations, advance our understanding of how the pattern features of a rival stimulus influence spatial interactions engaged by those features, thereby affecting qualitatively distinct aspects of binocular rivalry dynamics. Specifically, we have shown how contour collinearity in binocular rivalry influences two aspects of rivalry dynamics. (1) Traveling waves of dominance during state transitions occur on a relatively short time scale (i.e., a fraction of a second). (2) Perceptual dominance associated with spontaneous perceptual alternations occurs on a time scale up to an order of magnitude longer than that associated with traveling waves. Both of these aspects of rivalry are modulated by collinearity but in non-obvious ways as we have learned. To account for these counterintuitive results, we propose that pattern-dependent adaptation interacts with

collinear facilitation, and we have shown that this interaction can be accommodated within an extant model based on reciprocal inhibition among a network of units interconnected so as to promote varying degrees of collinear facilitation.

## Appendix A

### Latency of traveling waves

For statistical analyses, we estimated the latency of the waves from the switch function. The latency reflects the time at which perceptual states of both rival stimuli are equally likely. If traveling waves occur in response to all triggers, the latency would correspond to the time at which the mean perceptual state  $M(t)$  equals 0.5. However, if the periods of perceptual dominance differ for the two rival stimuli, and thus, one rival stimulus remains dominant for longer periods of time, the mean perceptual state will change accordingly over the entire trigger phase, implying that the latency identified based on the mean perceptual state  $M(t) = 0.5$  is not adequate. For this reason, a general procedure was devised in which the switch function was modeled by a sigmoid function,  $\alpha + \beta / (1 + \exp(-(\theta - \theta_T) / \sigma))$  in which  $\alpha$  equals  $M(0)$ , the mean perceptual state at trigger phase equals 0;  $\beta$  equals  $M(\pi) - M(0)$ , the difference between the mean perceptual states between the two trigger onsets;  $\theta_T$  is the threshold level of the trigger phase in the sigmoid function; and  $\sigma$  is the growth rate. Latencies of the traveling waves were identified individually by obtaining values of the threshold trigger phase  $\theta_T$  and transforming those values to the latency values in milliseconds by using the trigger period.

### Simulation details: Traveling waves

We conducted simulations using Matlab (Mathworks, MA) running on an Intel-based Macintosh computer with OS 10.5. The Euler method, a first-order numerical procedure for solving ordinary differential equations, was used for numerical integration with step size of 0.25 tu for 20,000 tu. Trigger period was set to 5000 tu starting from 2500 tu producing three waves associated with the carrier presented to the left eye and another three waves associated with the carrier presented to the right eye. Wave fronts shown in Figures 4b–4d were obtained by averaging these three wave fronts.

### Simulation details: Spontaneous perceptual alternations

The procedure used in Experiment 2 did not involve external, periodic perturbations to produce changes in

dominance state. To simulate spontaneous changes in dominance, we added a noise term  $\xi$  to Equation 2, such that the value  $P$  is given by

$$P_{Aj} = S_{Aj} - \eta_I \sum_{k=1}^N \varphi_{Bjk} I_{Bk} + \eta_E \sum_{k=1}^N \varepsilon_{Ajk} E_{Ak} + S_{Aj} \xi. \quad (\text{A1})$$

Noise values among the array of neurons are uncorrelated and are defined by a Gaussian distribution whose mean equals 0 and standard deviation equals 0.2. The amplitude of noise is scaled with the strength of the stimulus and noise values are updated every 25 tu. A single simulation is conducted for 240,000 tu and repeated four times for each condition (where a condition refers to a given combination of rival stimuli, extent of recurrent excitation, and pattern-dependent adaptation level). Each simulation required considerable time to complete, and to complete the simulations we reduced the size of the neuronal array from 40 to 20; this reduction in array size does not affect the results. The dominance duration for a given stimulus was defined as the duration during which all of the middle five model neurons (i.e., the units representing the monitoring region) were all specifying dominance of the same stimulus.

## Acknowledgments

This work was supported by grants from the U.S. National Institutes of Health (R01-EY013358, R01-EY016752, and P30-EY008126), and RB and SL were also supported by the WCU program administered by the National Research Foundation of Korea and funded by the Korean Ministry of Education, Science, and Technology (R32-10142).

Commercial relationships: none.

Corresponding authors: Min-Suk Kang and Randolph Blake. Emails: m.suk.kang@gmail.com; randolphblake@gmail.com. Address: Department of Psychology, Vanderbilt University, 111 21st Ave. South, 301 Wilson Hall, Nashville, TN 37240, USA.

## Footnotes

<sup>1</sup>To avoid confusion associated with the dual use of the term “suppression,” we will use the term “surround suppression” when referring to that form of contextual modulation and the term “suppression” on its own to refer to perceptual suppression during rivalry.

<sup>2</sup>Portions of data shown in Figure 3a (solid lines) are reproduced from a previous paper (Kang et al., 2009).

## References

- Alais, D., & Blake, R. (1998). Interactions between global motion and local binocular rivalry. *Vision Research*, *38*, 637–644.
- Alais, D., & Blake, R. (1999). Grouping visual features during binocular rivalry. *Vision Research*, *39*, 4341–4353.
- Alais, D., Lorenceau, J., Arrighi, R., & Cass, J. (2006). Contour interactions between pairs of Gabors engaged in binocular rivalry reveal a map of the association field. *Vision Research*, *46*, 1473–1487.
- Allman, J., Miezin, F., & McGuinness, E. (1985). Stimulus specific responses from beyond the classical receptive field: Neurophysiological mechanisms for local–global comparisons in visual neurons. *Annual Review of Neuroscience*, *8*, 407–430.
- Barlow, H. B., & Földiák, P. (1989). Adaptation and decorrelation in the cortex. In C. Miall, R. M. Durbin, & G. J. Mitchison (Eds.), *The computing neuron* (pp. 54–72). Wokingham, England: Addison-Wesley.
- Blake, R., & O’Shea, R. P. (2009). Binocular rivalry. In L. Squire (Ed.), *Encyclopedia of neuroscience* (vol. 2, pp. 179–187). Oxford, UK: Academic Press.
- Blake, R., & Overton, R. (1979). The site of binocular rivalry suppression. *Perception*, *8*, 143–152.
- Blakemore, C., Muncey, J., & Ridley, R. (1973). Stimulus specificity in the human visual system. *Vision Research*, *13*, 1915–1931.
- Blakemore, C., & Tobin, E. A. (1972). Lateral inhibition between orientation detectors in the cat’s visual cortex. *Experimental Brain Research*, *15*, 439–440.
- Bonneh, Y., & Sagi, D. (1999). Configuration saliency revealed in short duration binocular rivalry. *Vision Research*, *39*, 271–281.
- Brainard, D. (1997). The psychophysics toolbox. *Spatial Vision*, *10*, 433–436.
- De Valois, R., Albrecht, D., & Thorell, L. (1982). Spatial frequency selectivity of cells in macaque visual cortex. *Vision Research*, *22*, 545–559.
- Dörrenhaus, W. (1975). Musterspezifischer visueller wettstreit, *Naturwissenschaften*, *62*, 578–579.
- Ejima, Y., & Takahashi, S. (1985). Apparent contrast of a sinusoidal grating in the simultaneous presence of peripheral gratings. *Vision Research*, *25*, 1223–1232.
- Fahle, M. (1982). Binocular rivalry: Suppression depends on orientation and spatial frequency. *Vision Research*, *22*, 787–800.
- Field, D., Hayes, A., & Hess, R. (1993). Contour integration by the human visual system: Evidence for a local “association field”. *Vision Research*, *33*, 173–193.
- Fukuda, H., & Blake, R. (1992). Spatial interactions in binocular rivalry, *Journal of Experimental Psychology: Human Perception and Performance*, *18*, 362–370.
- Geisler, W., Perry, J., Super, B., & Gallogly, D. (2001). Edge co-occurrence in natural images predicts contour grouping performance. *Vision Research*, *41*, 711–724.
- Georges, S., Seriès, P., Frégnac, Y., & Lorenceau, L. (2002). Orientation dependent modulation of apparent speed: Psychophysical evidence. *Vision Research*, *42*, 2757–2772.
- Greenlee, M., Georgeson, M., Magnussen, S., & Harris, J. (1991). The time course of adaptation to spatial contrast. *Vision Research*, *31*, 223–236.
- Heeger, D. J. (1992). Normalization of cell responses in cat striate cortex. *Visual Neuroscience*, *9*, 181–197.
- Hubel, D., & Wiesel, T. (1962). Receptive fields, binocular interaction and functional architecture in the cat’s visual cortex. *The Journal of Physiology*, *160*, 106–154.
- Hubel, D., & Wiesel, T. (1968). Receptive fields and functional architecture of monkey striate cortex. *The Journal of Physiology*, *195*, 215–243.
- Ichihara, S., & Goryo, K. (1978). The effects of relative orientation of surrounding gratings on binocular rivalry and apparent brightness of central gratings. *Japanese Psychological Research*, *20*, 159–166.
- Kang, M.-S. (2009). Size matters: A study of binocular rivalry dynamics. *Journal of Vision*, *9*(1):17, 1–11, <http://www.journalofvision.org/content/9/1/17>, doi:10.1167/9.1.17. [PubMed] [Article]
- Kang, M.-S., & Blake, R. (2010). What causes alternations in dominance during binocular rivalry? *Attention, Perception & Psychophysics*, *72*, 179–186.
- Kang, M.-S., Heeger, D., & Blake, R. (2009). Periodic perturbations producing phase-locked fluctuations in visual perception. *Journal of Vision*, *9*(2):8, 1–12, <http://www.journalofvision.org/content/9/2/8>, doi:10.1167/9.2.8. [PubMed] [Article]
- Knapen, T., van Ee, R., & Blake, R. (2007). Stimulus motion propels traveling waves in binocular rivalry. *PLoS ONE*, *2*, e739.
- Kovács, I., & Julesz, B. (1993). A closed curve is much more than an incomplete one: Effect of closure in figure–ground segmentation. *Proceedings of the National Academy of Sciences of the United States of America*, *90*, 7495–7497.
- Kovács, I., Papathomas, T. V., Yang, M., & Fehér, A. (1996). When the brain changes its mind: Interocular grouping during binocular rivalry. *Proceedings of the*

*National Academy of Sciences of the United States of America*, 93, 15508–15511.

- Lankheet, M. J. M. (2006). Unraveling adaptation and mutual inhibition in perceptual rivalry. *Journal of Vision*, 6(4):1, 304–310, <http://www.journalofvision.org/content/6/4/1>, doi:10.1167/6.4.1. [PubMed] [Article]
- Lehky, S. R. (1988). An astable multivibrator model of binocular rivalry. *Perception*, 17, 215–228.
- Levelt, W. (1965). *On binocular rivalry*. Soesterberg, The Netherlands: Institution for Perception RVO-TNO.
- Li, W., Piëch, V., & Gilbert, C. (2006). Contour saliency in primary visual cortex. *Neuron*, 50, 951–962.
- Maffei, L., & Fiorentini, A. (1976). The unresponsive regions of visual cortical receptive fields. *Vision Research*, 16, 1131–1139.
- Mapperson, B., & Lovegrove, W. (1991). Orientation and spatial-frequency-specific surround effects on binocular rivalry. *Bulletin of the Psychonomic Society*, 29, 95–97.
- Meese, T. S., Georgeson, M. A., & Baker, D. H. (2006). Binocular contrast vision at and above threshold. *Journal of Vision*, 6(11):7, 1224–1243, <http://www.journalofvision.org/content/6/11/7>, doi:10.1167/6.11.7. [PubMed] [Article]
- Moreno-Bote, R., Rinzel, J., & Rubin, N. (2007). Noise-induced alternations in an attractor network model of perceptual bistability. *Journal of Neurophysiology*, 98, 1125–1139.
- Paffen, C. L. E., Tadin, D., te Pas, S. F., Blake, R., & Verstraten, F. A. J. (2006). Adaptive center-surround interactions in human vision revealed during binocular rivalry. *Vision Research*, 46, 599–604.
- Paffen, C. L. E., te Pas, S. F., Blake, R., Kanai, R., van der Smagt, M. J., & Verstraten, F. A. J. (2004). Center-surround interaction in visual motion processing during binocular rivalry. *Vision Research*, 44, 1635–1639.
- Pelli, D. (1997). The VideoToolbox software for visual psychophysics: Transforming numbers into movies. *Spatial Vision*, 10, 437–442.
- Rezec, A., Krekelberg, B., & Dobkins, K. R. (2004). Attention enhances adaptability: Evidence from motion adaptation experiments. *Vision Research*, 44, 3035–3044.
- Shapiro, A., Moreno-Bote, R., Rubin, N., & Rinzel, J. (2009). Balance between noise and adaptation in competition model in perceptual bistability. *Journal of Computational Neuroscience*, 27, 37–54.
- Smith, M. A. (2006). Surround suppression in early visual system. *Journal of Neuroscience*, 26, 3624–3625.
- Van Ee, R. (2009). Stochastic variations in sensory awareness are driven by noisy neuronal adaptation: Evidence from serial correlations in perceptual bistability. *Journal of the Optical Society of America A*, 26, 2612–2622.
- Wade, N., & de Weert, C. (1986). Aftereffects in binocular rivalry. *Perception*, 15, 419–434.
- Wade, N. J. (1974). The effect of orientation in binocular rivalry of real images and after-images. *Perception & Psychophysics*, 15, 227–232.
- Wade, N. J. (1975). Binocular rivalry between single lines viewed as real images and after-images. *Perception & Psychophysics*, 17, 571–577.
- Watanabe, K., Paik, Y., & Blake, R. (2004). Preserved gain control for luminance contrast during binocular rivalry suppression. *Vision Research*, 44, 3065–3071.
- Webb, B. S., Dhruv, N. T., Solomon, S. G., Tailby, C., & Lennie, P. (2005). Early and late mechanisms of surround suppression in striate cortex of macaque. *Journal of Neuroscience*, 25, 11666–11675.
- Wheatstone, C. (1838). Contributions to the physiology of vision—Part the first: On some remarkable, and hitherto unobserved, phenomena of binocular vision. *Philosophical Transactions of the Royal Society of London*, 128, 371–394.
- Whittle, P., Bloor, D., & Pocock, S. (1968). Some experiments on figural effects in binocular rivalry. *Perception & Psychophysics*, 4, 703–709.
- Wilson, H. (2005). Rivalry and perceptual oscillations: A dynamical synthesis. In D. Alais & R. Blake (Eds.), *Binocular rivalry* (pp. 317–335). Cambridge, MA: MIT Press.
- Wilson, H. (2007). Minimum physiological conditions for binocular rivalry and rivalry memory. *Vision Research*, 47, 2741–2750.
- Wilson, H., Blake, R., & Lee, S. (2001). Dynamics of travelling waves in visual perception. *Nature*, 412, 907–910.
- Xing, J., & Heeger, D. J. (2001). Measurement and modeling of center-surround suppression and enhancement. *Vision Research*, 41, 571–583.
- Yu, C., Klein, S. A., & Levi, D. M. (2002). Facilitation of contrast detection by cross-oriented surround stimuli and its psychophysical mechanisms. *Journal of Vision*, 2(3):4, 243–255, <http://www.journalofvision.org/content/2/3/4>, doi:10.1167/2.3.4. [PubMed] [Article]